TrackMAC: An IEEE 802.11ad-Compatible Beam Tracking-Based MAC Protocol for 5G Millimeter-Wave Local Area Networks

Bharadwaj Satchidanandan[1], Simon Yau[1], P. R. Kumar, *Fellow, IEEE*[1],
Ahsan Aziz[2], Amal Ekbal[2], and Nikhil Kundargi[2]

[1]Electrical and Computer Engineering, Texas A&M University, College Station
[2]National Instruments, Austin

***Abstract*—This paper presents a novel framework for MAC design for millimeter-wave (mm-wave) mobile wireless networks. Specifically, we consider an infrastructure wireless network in which both the Access Point (AP) and the mobile stations (STAs) communicate in the 60GHz band. In order to overcome the high path loss that is characteristic of mm-wave frequencies, both the transmitter as well as the receivers employ beamforming and use highly directional beams for transmission and reception. In such a scenario, traditional Medium Access Control (MAC) protocols such as CSMA/CA, which rely on the omni-directional nature of transmissions, may no longer be viable for efficient medium access control. It is necessary for the AP to know the directions that the associated STAs are in so that it can steer its transmissions to an intended receiver in that receiver's direction. In light of this, we propose TrackMAC, a directional MAC protocol that (i) has the property that it continuously tracks the direction of every associated station which, in general, is mobile, and (ii) can be implemented squarely within the specifications of the IEEE 802.11ad standard for mm-wave Wireless Local Area Networks (WLAN). The efficacy of the proposed architecture is demonstrated using computer simulations.**

I. Introduction

As the usage of wireless networks continues to expand, various stakeholders across the board are developing new technologies to improve the throughput and latency of next-generation wireless networks. One of the key enabling technologies of 5G wireless networks is to operate in bandwidths between 30 GHz and 300 GHz, also known as millimeter wave (mm-wave) bands. The vast amount of spectrum available in the mm-wave bands allows for significantly higher bandwidth that could potentially improve the network performance by orders of magnitude. However, developing wireless technology in this band is not without challenges. One key challenge is the high attenuation at mm-wave frequencies. Specifically, it follows from the Friis formula

$$P_R = P_T G_R G_T (\frac{\lambda}{4\pi r})^2,$$

This material is based upon work partially supported by NSF under Contract Nos. CNS-1646449, CCF-1619085 and Science & Technology Center Grant CCF-0939370, and the U.S. Army Research Office under Contract No. W911NF-15-1-0279.

that in free space, the path loss of the signal scales as $\frac{1}{f^2}$ where f is the frequency of the transmitted signal. In the above, P_T and P_R denote the transmitted and received signal powers respectively, G_T and G_R denote the transmit and receive antenna gains respectively, r denotes the distance between the transmitter and the receiver, and $\lambda = \frac{c}{f}$ is the wavelength of the transmitted signal. This in turn implies that for a given transmit and receive antenna gains, the signal power attenuation at 60GHz, which is the frequency band of interest in this paper, is about 27dB higher than that at 2.5GHz.

In order to overcome this high attenuation, it is imperative to increase the antenna gains G_R and G_T. Fortunately, the antenna dimensions scale inversely with the operating frequency and consequently, embedding tens to even hundreds of antennae in a small form factor becomes feasible at 60GHz, allowing one to perform transmit and receive beamforming, thereby increasing the antenna gains in certain directions [1]–[9]. Indeed, the antenna gains G_T and G_R for a given antenna aperture scale as f^2, and consequently, one now obtains a power attenuation that is 27dB *lower* at 60GHz as compared to 2.5GHz [10]. The combination of high bandwidth and higher received power at 60GHz makes mm-wave communications an ideal technology to achieve multi-gigabit-per-second wireless communications which has applications in several domains including wireless backhauling and real-time high-definition video streaming.

Employing highly directional beams for transmission and reception introduces certain novel challenges for MAC design. Specifically, highly directional beams introduce the problem of deafness described in [11], and traditional MAC protocols such as CSMA/CA, which rely on the omnidirectional nature of transmissions and receptions, may no longer be effective in orchestrating the medium access. Secondly, the fact that the nodes are directional necessitates the transmitter to keep track of where every STA is, which could be a significant challenge when the STAs are mobile. Note that in such a scenario, it is not only the position of the nodes in the system that affects the network performance, but also their orientations. In other words, as the directional STAs physically move or rotate in a cell, the AP has to track these changes and adapt its transmissions and receptions accordingly. Likewise, each STA has to adapt its transmissions and receptions in response to its own displacement and rotation. Certain other challenges such as blockage also feature in millimeter-wave bands which the MAC protocol has to take into account.

In light of the above challenges unique to millimeter-wave networks, it becomes necessary to develop new directional MAC protocols for these networks which address the problems of deafness, mobility, and blockage. In this paper, we present TrackMAC, a directional MAC protocol which has certain important beneficial features as described below.

First, TrackMAC allows for both scheduled service periods as well as contention-based channel access, and does so while taking into account the mobility of the nodes, both translational as well as rotational, based on a conservative estimate of how quickly a node can move and rotate. In this context, we introduce the notion of *Topological Coherence Time* T_{tc} of a directional wireless network. Roughly speaking, this is the maximum duration during which the topology of the network remains "constant." This quantity depends primarily on the mobility of the nodes in the network, but could also be influenced by the beamwidths of the antennae. We discuss this in more detail in the following sections.

One of the key bottlenecks affecting the performance of a mm-wave network is the delay associated with discovering the relative position and orientation between the AP and a STA. To address this issue, TrackMAC is designed in such a manner that with a small overhead, the need for constant rediscovery of the network topology by the centralized scheduler or AP is eliminated.

Importantly, as we show in Section IV, TrackMAC has a significant architectural advantage: It can be implemented squarely within the framework of the IEEE 802.11ad standard. Specifically, TrackMAC can be realized by reprogramming *only the scheduling layer* of an IEEE 802.11ad network stack.

While the issue of blockage of millimeter waves by objects such as the human body, office furniture, etc is not explicitly addressed in this paper, the features of protocols that address it, such as multihop relaying [10], can well be implemented within the framework of TrackMAC in a relatively straightforward fashion.

In summary, the contributions of this paper are three-fold:

1) The introduction of the notion of topological coherence time of a directional wireless network, which is potentially a key parameter for designing efficient directional MAC protocols.
2) TrackMAC, a directional MAC protocol which takes into account the topological coherence time, the directionality of the nodes, and which continually tracks every associated STA with a small overhead, thereby removing the need for constant rediscovery of mobile nodes.
3) Implementation of TrackMAC within the specifications of the IEEE 802.11ad standard.

The rest of the paper is organized as follows. Section II gives an account of related work in this area, and also outlines the key distinctions between these efforts and our work. Section III describes TrackMAC, the proposed MAC protocol. Section IV outlines certain key features of the IEEE 802.11ad standard, and also describes how TrackMAC can be implemented within the specifications of the standard by reprogramming only the scheduling layer of the network. Section V presents some simulation results, and Section VI contains some concluding remarks.

II. Related Work

Before mmWave was widely viewed as a feasible technology for increasing usable spectrum for wireless networks, there had been several studies examining the use of directional MAC protocols to improve spatial reuse for sub-6GHz ad hoc wireless networks [12]–[21]. However, these papers do not consider mobility of the nodes and consequently, may not perform well in an indoor scenario with mobile nodes. In [13], [16], [22], [23], the authors focus on directional MAC protocols for ad hoc networks. However, protocols designed for ad hoc networks can incur significant overhead and cause significant degradation to the efficiency of an infrastructure wireless network. Furthermore, these protocols were not designed for mm-wave bands, and they rely on assumptions that do not apply in these bands.

In [24], the authors briefly mention handling of mobility in a Wide Area Network (WAN) but do not consider how mobility affects the scheduling of nodes. Reference [25] proposes a MAC protocol that works in mobile scenarios and also details how the location of the stations are updated. However, this work is not based on the IEEE 802.11ad standard, and so, it may not be possible to implement it within the specifications of the standard. Similarly, in [26], the authors develop an algorithm for avoiding blockage and dealing with mobility. However, they require all associated STAs to inform the AP of the transmission rates between them and all other STAs every 10ms (for the scheduling decisions), which may not be compatible with IEEE 802.11ad. Full details of the IEEE 802.11ad specifications can be found in [27].

Reference [28] provides a directional MAC implementation on top of the current IEEE 802.11ad standard. However, like some of the papers cited above, it too does not consider mobility of the nodes.

III. Design Methodology of TrackMAC

Consider a mm-wave infrastructure wireless network as shown in Figure 1. The role of the AP is to (i) communicate with the STAs already associated with it, and (ii) enable new nodes in its vicinity to join the network by associating them with it. The latter is commonly known as Initial Access (IA). In what follows, we describe the protocol for both the IA phase as well as for the data transmission phase.

A. Topological Coherence Time

One of the key parameters that determines the exact design of the proposed MAC protocol is the topological coherence time, denoted by T_{tc}. Akin to the notion of the coherence time of a wireless channel, the topological coherence time

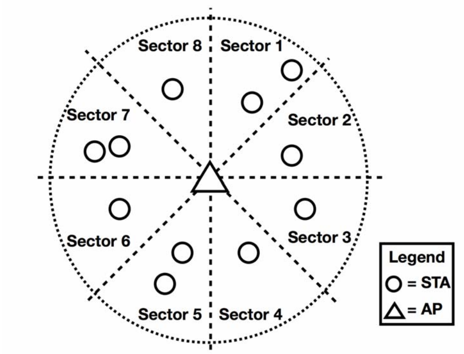

Fig. 1. A mm-wave network operating in infrastructure mode

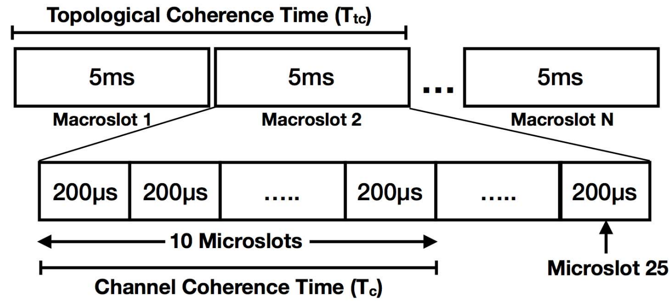

Fig. 2. Division of time into Macroslots, of Macroslots into Microslots

is a measure of how fast the network topology changes. To illustrate this notion in a very simple context, consider a mm-wave network with just one AP and one STA. Suppose also that each of these nodes is equipped with an antenna array with a 3dB beamwidth of, say, 10°. For simplicity, suppose that there is only one dominant path from the AP to the STA, and that it is the Line-of-Sight (LoS) path. Let the AP's beam and the STA's beam be perfectly aligned at time $t = 0$. As time progresses, the STA moves and rotates, so that the STA's beam becomes misaligned with respect to the AP's beam. Consequently, the link gain $G_T G_R$, where G_T and G_R are the transmit and receive antenna gains respectively, fluctuates from its peak value. The topological coherence time is defined as the time t until which any link's gain degrades no more than 3dB from its peak value. Clearly, in this example, the topological coherence time is a function of the maximum rotational and translational speeds of the STAs. For instance, if the STAs are assumed to be stationary and the maximum rotational speed of the STAs is 360 degrees/s, a very conservative estimate, then, for a 3dB beamwidth of 10°, the topological coherence time is of the order of $\frac{5}{360} \approx 14$ms.

In a more general scenario, the topological coherence time may not be expressible explicitly in terms of just the mobility parameters of the STAs, but nevertheless, it is a quantity that, like channel coherence time, is measurable in an order of magnitude sense.

B. TrackMAC: A Novel Directional MAC Protocol

In what follows, we describe the TrackMAC protocol as well as the methodology by which the parameters of the protocol are designed. For the sake of exposition, we make use of a running example to illustrate the design methodology.

In the proposed MAC protocol, time is divided into a series of slots known as "macroslots." The duration of each macroslot, denoted by T_M, is set to be $T_M = \frac{T_{tc}}{p}$, where $p \geq 2$ is an arbitrary design parameter. The rationale for constraining $p \geq 2$ will become apparent shortly. In our running example, we take $p = 2$. Also for our example, we assume T_{tc} to be of the order of 10ms, so that the macroslot duration is $T_M = 5$ms.

Now, depending on the maximum number of STAs that are to be supported by an AP, each macroslot is further subdivided into several slots known as "microslots." Specifically, if N is the maximum number of STAs that are to be associated with an AP, then, each macroslot is divided into N microslots, so that each microslot extends for a duration of $T_m = \frac{T_M}{N}$. In our example, we suppose that the AP is not expected to serve more than $N = 25$ STAs at a time, so that each macroslot consists of 25 microslots. It follows that each microslot extends to a duration of $T_m = 200\mu$s. This structure of macroslots and microslots is illustrated in Fig. 2.

Now, during the data transmission phase (as opposed to IA phase), each STA associated with the AP is scheduled by the AP in certain microslots. The only constraint for the AP is that it schedules each STA at least once in each macroslot. Note that since by design the time difference between any two microslots belonging to adjacent macroslots is lesser than the topological coherence time, the AP knows the direction in which it has to point its beam in each microslot in order to communicate with the intended STA. Once the link is established during a microslot, the AP and the STA consume some training overhead time to refine their beam directions. This ensures that the STA never strays too far away from the stored direction in the AP's direction table, and can always be tracked as long as the AP schedules the STA at least once in each macroslot. Subject to just this one constraint, the AP can schedule the STAs in any manner that maximizes the network utility. In fact, as long as the AP satisfies this scheduling constraint, it can also allocate certain microslots in each macroslot for contention-based access (CBAP). Any contention protocol designed for directional nodes can be employed in this time period. Finally, the ACK frames are transmitted by the STAs at the end of each microslot using time division duplexing.

Next, we describe and evaluate the MAC overhead required for the functioning of TrackMAC. In addition to beam refinement, training overhead time should be and is allotted in each microslot for the purposes of (i) symbol timing recovery, (ii) channel estimation, and (iii) frame synchronization. We now estimate the amount of overhead required for each of these.

Based on indoor channel measurement studies at mm-wave frequencies, the delay spread of the channel in a typical indoor office-like environment is at most 500ns [29]. This mandates that the channel estimation (CE) pilots be at least 500ns in duration. While allocating a CE pilot duration that is an order of magnitude larger than the channel delay spread may be preferable for smoothing the channel estimate in the presence of noise, any allocation higher than the delay spread is sufficient for estimating the channel impulse response. While in our running example we allocate 5μs for CE pilots, which is an order of magnitude larger than the delay spread of the channel, an allocation of about 650ns would be in adherence with the 802.11ad standard as explained in the next section. Next, we examine how often within a microslot the channel has to be estimated. This depends on the channel coherence time. For a typical indoor speed of about $v = 1.5$m/s, the doppler spread D of the channel at 60GHz is about $D = \frac{f_c v}{c} = 300$Hz, corresponding to a channel coherence time that is of the order of $\frac{1}{D} = 3.33$ms. Since this an order of magnitude larger than the microslot duration, it is sufficient to allocate just 5μs per microslot out of the 200μs available for channel estimation.

Typically, standard sequences, such as Golay sequence or Zadoff-Chu sequence, of various possible lengths are chosen as training symbols for timing recovery and frame synchronization owing to certain autocorrelation properties that they exhibit. For example, as shown in [30] in the context of mm-wave links, a sequence length of 2048 symbols provides robust symbol timing recovery. We use the same training length in our running example. Consequently, for a symbol duration of $T_s = \frac{1}{W} = 0.46$ns that is typical in the 60GHz band for a bandwidth $W = 2.16$GHz (in adherence with the IEEE 802.11ad standard), this translates to a pilot duration for timing recovery of about 1μs. Finally, while training symbol duration for beam refinement can also be chosen freely, in our running example, we allocate between 10μs and 15μs for this, which again is in adherence with 802.11ad.

Adding all of the above pilot durations, we obtain a total overhead of approximately 20μs per microslot, which leaves about 180μs per microslot for transmission of the MAC payload. This in turn translates to a total MAC overhead of about 10%.

In addition to the above training overheads, some specified time $t_{control}$ may be allocated in each microslot for exchanging control information. Although we don't do this in this paper in order to adhere with 802.11ad specifications, in general this could be done, and during this time, the AP and the STA could exchange information such as queue backlog, packet deadlines, channel quality index, the microslot in the next macroslot in which the STA is scheduled, etc. Note that this allows the AP to schedule the STAs adaptively every macroslot based on their queue backlogs, required deadlines, etc.

In order to allow for initial access, we designate one macroslot periodically as "IA macroslot." In our example, we suppose that one macroslot in every twenty macroslots is designated as an IA macroslot. In an IA macroslot, the AP transmits a beacon in one of the pre-defined sectors using a low-order modulation scheme such as BPSK and a low rate code. A STA that wishes to associate with the network configures its antenna in a quasi-omnidirectional mode similar to the IA procedure of IEEE 802.11ad described in the next section. While the quasi-omnidirectional reception leads to low received SNR, the fact that the beacon, which is only a few bits in length (not more than 1000 bits in 802.11 systems), is transmitted at a very low rate enables the STA to reliably decode the beacon. Once the beacon is decoded, the AP and the STA perform the beamforming procedure specified in the 802.11ad standard [27] to align their beams. Some specified duration of the IA macroslot is also allocated to communicate the schedule of every associated STA until the next IA macroslot.

We do not specify a duration for the IA phase, but the longer this period is, the higher the probability of an STA being associated with the AP. Consequently, more STAs can be associated with the AP during a single IA phase. On the other hand, if this period is set too short, an STA may require many IA phases before finally being associated with the AP (or reassociated with the AP if the AP fails to track the STA). Once the STA associates with the AP, the latter stores the location of the newly associated STA in its direction table, and also specifies its schedule till the next IA Macroslot.

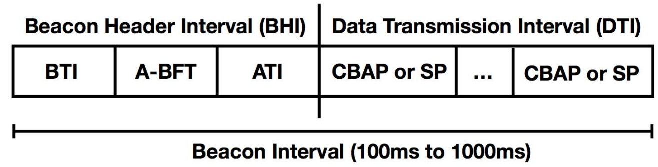

Fig. 3. Structure of a Beacon Interval

IV. Implementation of TrackMAC within the IEEE 802.11ad Specifications

Before we describe how TrackMAC can be implemented within the specifications of the 802.11ad standard, we provide a brief overview of certain key specifications of the standard. Some basic familiarity with the standard is assumed of the reader in this section. A more comprehensive description of the standard can be found in [31], [32], and the standard itself can be found in [27].

Consider a Basic Service Set (BSS) operating in infrastructure mode – the AP is connected to all other STAs. Similar to legacy 802.11 standards, the 802.11ad divides the time axis into Beacon Intervals (BI). While the exact duration of a BI can be chosen by the system designer, it has to be chosen in the range of 100ms and 1000ms. In most practical deployments, it is chosen to be in the order of about 100ms.

Fig. 3 illustrates the structure of a BI. As shown, each BI is composed of two phases - the Beacon Header Interval (BHI) and the Data Transmission Interval (DTI). The BHI duration is not specified in the standard, and is free to be chosen by the system designer. Typically, the BHI is in the order of a few milliseconds, and the DTI consumes the bulk of the BI. In our example, we dedicate about 2ms for BHI, and about 98ms for DTI.

The BHI is further subdivided into three phases - the Beacon Transmission Interval (BTI), followed by an Associa-

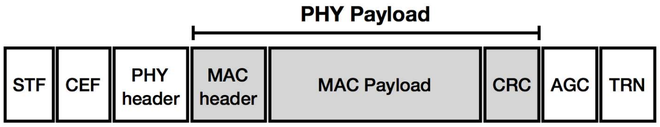

Fig. 4. 802.11ad PHY Packet Structure

tion Beamforming Training (A-BFT) interval, and finally the Announcement Time Interval (ATI). During the BTI, the AP transmits a beacon directionally in certain predefined sectors as mentioned before using the Modulation and Coding Scheme 0 (MCS 0). This is the lowest rate MCS scheme defined in the 802.11ad standard, and offers maximum error protection. This MCS is typically used prior to beamforming to exchange critical control information in a robust fashion [31], but never for data transmission since it is severely limited in terms of data rate.

The A-BFT period is used for associating and beamforming training of the new STAs. Specifically, during the A-BFT phase, the AP and the STA transmit and receive pilot sequences in different predefined sectors to converge on the best transmit and receive sectors. While these sectors, being predefined, are quantized and provide coarse beamforming, finer beam refinement could also be performed to converge on optimal beam directions.

Finally, during the ATI, the AP informs every associated STA the schedule during DTI. Specifically, during DTI, some time periods can be dedicated for servicing specific STAs, while other time periods could be designated for contention-based channel access. Whatever the schedule is, the AP informs each associated STA of the schedule.

The DTI begins after the ATI. Each DTI can support multiple data transmissions to different STAs, and they can be scheduled in any fashion by the scheduling layer. The standard supports a hybrid access method, i.e., both scheduled and contention-based transmissions are supported during the DTI.

Fig. 5 illustrates how TrackMAC can be implemented within the 802.11ad framework. Specifically, with respect to the MAC layer, the IA macroslots in our protocol essentially are designed in such a way that microslots 1 thru 10 of the IA macroslots are designated for BHI. This translates to a BHI duration of 2ms (recall that each microslot is 200μs long). To attain a BI duration of 100ms, one IA macroslot is interleaved between every 19 macroslots (recall that a macroslot is 5ms long). The overlay of macroslots on an 802.11ad BI is shown in Fig. 5.

Finally, a physical layer packet of 802.11ad can be of three types, viz., control PHY, single-carrier PHY (SC-PHY), and OFDM PHY. All physical-layer packets of 802.11ad have the same set of fields - the Short Training Field (STF) for signal detection and symbol timing recovery, the Channel Estimation Field (CEF), the PHY Header field which contains all necessary information to decode the MAC payload, the MAC payload, and finally the beamforming training field

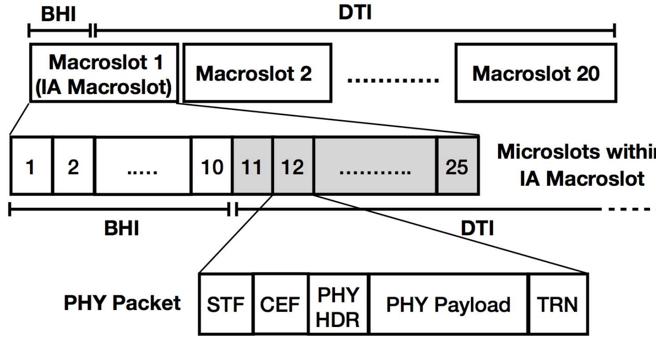

Fig. 5. Overlay of 802.11ad PHY packets on microslots and macroslots on 802.11ad BI

(TRN). It is only the duration of each field and the MCS used in the MAC payload that is different for different PHY packet types. The structure of a PHY packet with different fields marked is shown in Fig. 4.

The beamforming training field of a PHY packet consists of pilot sequences that are transmitted by the AP in different sectors adjacent to the direction in which the MAC payload is transmitted. The number of sectors along which training sequences are to be transmitted can range from 0 to 64 in multiples of 4.

Also shown in Fig. 5 is the overlay of PHY packets used in 802.11ad on the microslots. Specifically, a PHY packet of 802.11ad has all the fields present in a microslot defined in TrackMAC. Furthermore, the duration of the different fields of the 802.11ad PHY packet is in conformity with those of a microslot. The STF of the 802.11ad SC-PHY packet, which serves the purpose of pilot symbols for symbol timing recovery, is about 1.2μs long, which is the about the same duration alloted in a microslot for timing recovery. Similarly, the channel estimation field of an 802.11ad SC-PHY packet is 645.12ns, which can be mapped to the channel estimation pilots in a microslot. Finally, the beamforming training fields in 802.11ad can range anywhere from a little more than 10μs to about 180μs depending on the number of sectors that pilot symbols should be transmitted in. However, note that since the time difference between two consecutive channel accesses of a STA is never more than the topological coherence time in TrackMAC, it is enough for beamforming training sequences to be transmitted in just $S = 4$ sectors adjacent to the direction of payload transmission, for typical beamwidths used. For this choice of S, the duration of the training field extends to a little more than 10μs in 802.11ad, which conforms to the beamforming training field duration in a microslot defined in TrackMAC.

The aforementioned mapping ensures that the scheduling algorithm running on top of an 802.11ad MAC layer organizes medium access, as well as the physical layer transmissions, are in adherence with both TrackMAC and the 802.11ad specifications. The scheduling algorithm needs to only satisfy the constraint that every STA is scheduled at least once in every macroslot in order to track every mobile STA associated

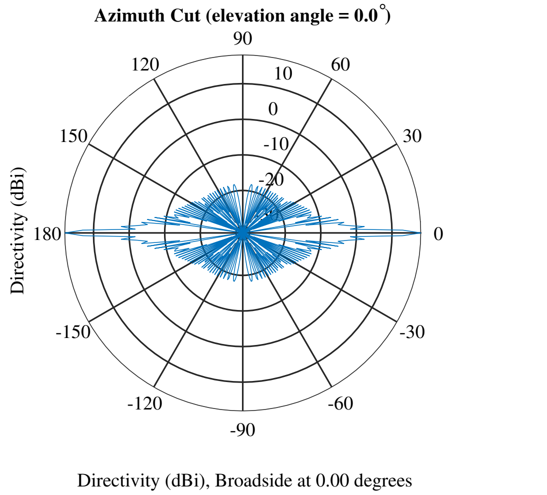

Fig. 6. Azimuth pattern of a $\lambda/2$-spaced 64-element ULA at 60.48GHz

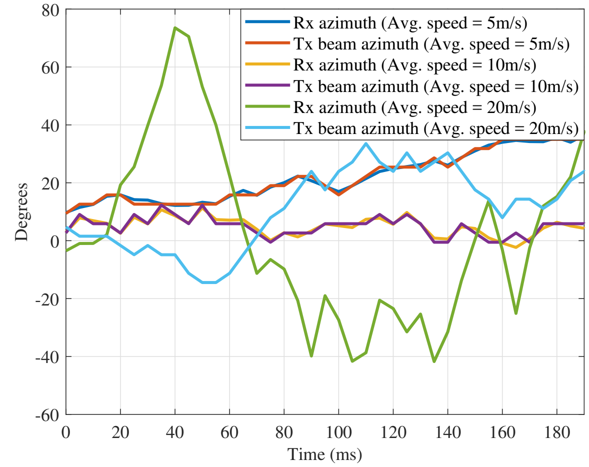

Fig. 7. Tracking performance of the AP for three different STA translational speeds (5m/s, 10m/s, and 20m/s). Plotted against time are (i) the azimuth direction of a particular randomly chosen STA out of the 25 associated STAs, and (ii) the azimuth direction in which the AP points its transmit beam when it communicates with that particular STA. For STA translational speeds of 5m/s and 10m/s, the AP is able to track the movement of the STA, whereas for STA translational speed of 20m/s, the AP is unable to do so.

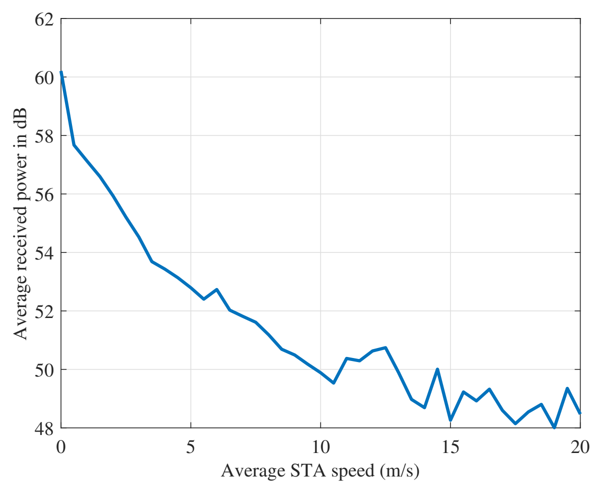

Fig. 8. Average received signal power vs. translational speed of STAs. The abscissa denotes the avg. speed at which the STAs move, and the ordinate denotes the avg. power level at which the MAC payload is received. The averaging is performed over STAs.

with it.

V. Simulation Results

As described in Section III, an important feature of the proposed scheduling framework or the TrackMAC is its ability to track every mobile station that is associated with it. One of the primary purposes of our simulations is to evaluate the tracking efficacy of TrackMAC. Towards this, we evaluate in our simulations (i) the tracking performance of the AP when it employs the proposed scheduling algorithm, and (ii) the average received signal strength for different mobility parameters, a key physical layer performance metric.

In our simulations, each node (AP or STA) is equipped with a Uniform Linear Array (ULA) of 64 elements, which gives it the ability to beamform. The inter-element spacing in the ULA is set to $\lambda/2 = 25$mm, where $\lambda = \frac{c}{f_c}$ is the carrier wavelength. Fig. 6 shows the azimuth pattern of such an array. The 3dB beamwidth of the array is about $1.6°$.

We simulate the system in a "fully loaded" condition, i.e., the number of STAs associated with the AP equals the number of microslots. The number of microslots is set to 25 in our simulations, resembling the design in our running example. Also, the network is simulated for a duration of 200ms which equals two beacon intervals.

In a LoS indoor environment and for typical translational and rotational velocities of users, the dominant factor that determines the topological coherence time is the rotational speed of the STAs. Motivated by this, we first present the simulation results of a scenario in which the STAs are stationary but rotate at a speed chosen uniformly at random with a given upper bound. In this case, the receiver uses the training fields (TRN) to steer its beam in the direction of best received signal strength. If the receiver, in addition to rotating about its position, also moves, then the AP has to track the STAs. In a second scenario, we simulate this case with the STAs having their receive beams directed towards the transmitter, but are mobile, thereby requiring the AP to track them as they move in the azimuth. In this case, the STAs move at a speed chosen uniformly at random with a given upper bound.

Fig. 7 and Fig. 8 illustrate the tracking performance of the AP as the receiver's azimuth varies. The receiver is assumed to be beamformed towards the AP, and the beamforming training field transmitted in the PHY packet of the AP consists of training symbols for four sectors. Since the 3dB beamwidth of the antenna is about $1.6°$, the training sectors of the PHY packet are chosen to be $\pm 1.6°$ and $\pm 3.2°$ relative to the direction in which the payload is transmitted. Fig. 9 shows the array pattern when the antenna beam is steered using steering

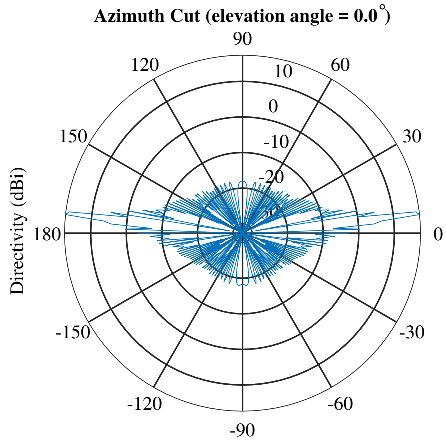

Fig. 9. Azimuth pattern of the ULA with steering weights corresponding to 3.2° azimuth

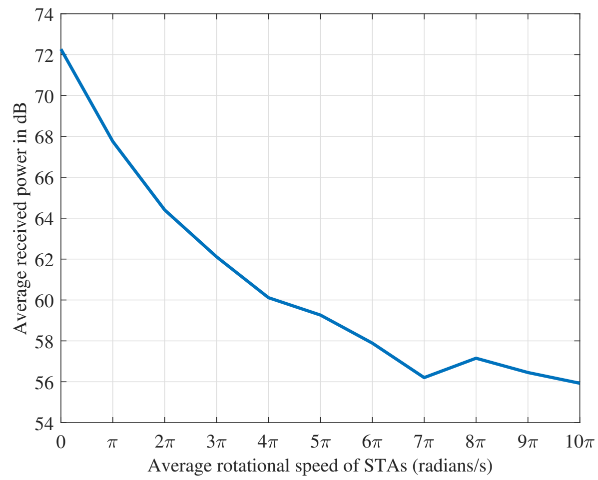

Fig. 10. Average received signal power vs. rotational speed of STAs. The abscissa denotes the avg. speed at which the STAs rotate, and the ordinate denotes the avg. power level at which the MAC payload is received. The averaging is performed over STAs.

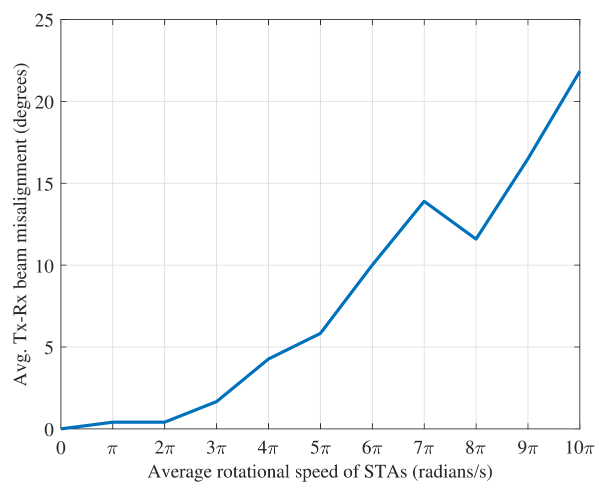

Fig. 11. Tracking performance of AP and STAs for different rotational speeds. The abscissa denotes the avg. rotational speed of the STAs and the ordinate represents the angle between the directions of the transmitter's beam and the intended receiver's beam, averaged over both STAs and time. The network was simulated for one beacon interval.

weights corresponding to 3.2° in the azimuth. It can be seen from Fig. 7 that TrackMAC is able to track translational speeds that are fairly high for indoor scenarios (upwards of 10m/s), and deteriorates as the STA speed becomes larger and larger. Fig. 8 plots the average power level at which the MAC payload is received a function of STA speed. Specifically, if $\mathbf{x}_{m,n}$ denotes the signal received by STA m, $m = 1, ..., 25$ during macroslot n, $n = 1, ..., 40$ (the network is simulated for 2 BIs which equals 200ms or equivalently, 40 macroslots), then the figure plots $\frac{1}{25}\sum_{m=1}^{25}\frac{1}{40}\sum_{n=1}^{40}\frac{||\mathbf{x}_{m,n}||^2}{T}$. Here, T is the length of MAC payload during a microslot. In our simulations, $T = 41768$ octets. Since the focus is on simulating the MAC protocol, no PHY aspects such as small-scale fading or noise are simulated.

Fig. 11 and Fig. 10 illustrate the tracking performance of the protocol in the presence of STA rotation. The AP is now assumed to be beamformed in the direction of STAs. As in the previous set of simulations, here too the beamforming training field of the STAs consist of training symbols for sectors $\pm 1.6°$ and $\pm 3.2°$ relative to the direction in which the payload is transmitted. Fig. 11 shows the average misalignment between the AP and the STA's beams as a function of the STA's rotational speed, and Fig. 10 plots the average received payload signal power in a microslot. For nominal rotational velocities expected of users, the misalignment between the beams, and also the average received signal power, are not severely degraded.

VI. Conclusions and Future Work

This paper presented TrackMAC, a directional MAC protocol for indoor mm-wave infrastructure wireless networks with mobile users. The high directionality of the nodes in such networks necessitates the AP and each station to track each other over time, preferably with small overheads, in order to obtain sufficient link budget in mm-wave bands. A protocol that achieves this was presented, and the required MAC overheads were analyzed. It was shown that for typical indoor speeds, tracking could be achieved with a MAC overhead of about 10%. The tracking performance was evaluated using computer simulations. Finally, it was shown that TrackMAC can be implemented squarely within the specifications of the IEEE 802.11ad standard developed for mm-wave wireless local area networks. This is achieved by employing a certain class of scheduling algorithms in the scheduling layer of an 802.11ad network stack. Future work includes prototyping TrackMAC on a mm-wave platform and evaluating its performance.

REFERENCES

[1] J. M. Gilbert, C. H. Doan, S. Emami, and C. B. Shung, "A 4-Gbps uncompressed wireless HD A/V transceiver chipset," in *IEEE Micro*, vol. 28, no. 2, 2008, pp. 56–64.

[2] S. Piersanti, L. A. Annoni, and D. Cassioli, "Millimeter waves channel measurements and path loss models," in *2012 IEEE International Conference on Communications (ICC)*, 2012, pp. 4552–4556. [Online]. Available: http://ieeexplore.ieee.org/lpdocs/epic03/wrapper.htm?arnumber=6363950

[3] Z. Pi and F. Khan, "An introduction to millimeter-wave mobile broadband systems," *IEEE Communications Magazine*, vol. 49, no. 6, pp. 101–107, 2011.

[4] E. Ben-Dor, T. S. Rappaport, Y. Qiao, and S. J. Lauffenburger, "Millimeter-wave 60 GHz outdoor and vehicle AOA propagation measurements using a broadband channel sounder," in *GLOBECOM - IEEE Global Telecommunications Conference*, 2011.

[5] T. S. Rappaport, E. Ben-Dor, J. N. Murdock, and Y. Qiao, "38 GHz and 60 GHz angle-dependent propagation for cellular & peer-to-peer wireless communications," in *IEEE International Conference on Communications*, 2012, pp. 4568–4573.

[6] T. S. Rappaport, S. Sun, R. Mayzus, H. Zhao, Y. Azar, K. Wang, G. N. Wong, J. K. Schulz, M. Samimi, and F. Gutierrez, "Millimeter wave mobile communications for 5G cellular: It will work!" *IEEE Access*, vol. 1, pp. 335–349, 2013.

[7] T. E. Bogale and L. B. Le, "Massive MIMO and mmWave for 5G Wireless HetNet: Potential Benefits and Challenges," *IEEE Vehicular Technology Magazine*, vol. 11, no. 1, pp. 64–75, 2016.

[8] G. R. Maccartney and T. S. Rappaport, "73 GHz millimeter wave propagation measurements for outdoor urban mobile and backhaul communications in New York City," in *2014 IEEE International Conference on Communications, ICC 2014*, 2014, pp. 4862–4867.

[9] T. S. Rappaport, G. R. MacCartney, M. K. Samimi, and S. Sun, "Wideband millimeter-wave propagation measurements and channel models for future wireless communication system design," *IEEE Transactions on Communications*, vol. 63, no. 9, pp. 3029–3056, 2015.

[10] S. Singh, F. Ziliotto, U. Madhow, E. M. Belding, and M. Rodwell, "Blockage and directivity in 60 GHz wireless personal area networks: From cross-layer model to multihop MAC design," *IEEE Journal on Selected Areas in Communications*, vol. 27, no. 8, pp. 1400–1413, 2009.

[11] S. Singh, R. Mudumbai, and U. Madhow, "Distributed coordination with deaf neighbors: Efficient medium access for 60 GHz mesh networks," *Proceedings - IEEE INFOCOM*, 2010.

[12] M. Takai, J. Martin, R. Bagrodia, and A. Ren, "Directional carrier sensing for directional antennas in mobile ad hoc networks," *International symposium on Mobile ad hoc networking & computing*, vol. 3, pp. 183–193, 2002.

[13] V. Shankarkumar and N. Vaidya, "Medium access control protocols using directional antennas in ad hoc networks," in *Proceedings IEEE INFOCOM 2000. Conference on Computer Communications. Nineteenth Annual Joint Conference of the IEEE Computer and Communications Societies (Cat. No.00CH37064)*, 2000, pp. 13–21. [Online]. Available: http://ieeexplore.ieee.org/xpl/freeabs_all.jsp?arnumber=832169

[14] Y.-B. K. Y.-B. Ko, V. Shankarkumar, and N. Vaidya, "Medium access control protocols using directional antennas in ad hoc networks," *Proceedings IEEE INFOCOM 2000. Conference on Computer Communications. Nineteenth Annual Joint Conference of the IEEE Computer and Communications Societies (Cat. No.00CH37064)*, vol. 1, no. c, pp. 13–21, 2000. [Online]. Available: http://ieeexplore.ieee.org/lpdocs/epic03/wrapper.htm?arnumber=832169

[15] A. Nasipuri, S. Ye, J. You, and R. E. Hiromoto, "A MAC Protocol for Mobile Ad Hoc Networks Using Directional Antennas," *Proc. of IEEE INFOCOM*, pp. 1214–1219, 2000.

[16] R. R. Choudhury, X. Yang, N. H. Vaidya, and R. Ramanathan, "Using directional antennas for medium access control in ad hoc networks," *Proceedings of the 8th annual international conference on Mobile computing and networking - MobiCom '02*, p. 59, 2002. [Online]. Available: http://portal.acm.org/citation.cfm?doid=570645.570653

[17] M. Gong and R. Stacey, "A directional CSMA/CA protocol for mmWave wireless PANs," *Wireless . . .*, pp. 1–6, 2010. [Online]. Available: http://ieeexplore.ieee.org/lpdocs/epic03/wrapper.htm?arnumber=5506128

[18] M. X. Gong, D. Akhmetov, R. Want, and S. Mao, "Directional CSMA/CA protocol with spatial reuse for mmWave wireless networks," *GLOBECOM - IEEE Global Telecommunications Conference*, pp. 1–5, 2010.

[19] Q. Chen, X. Peng, J. Yang, and F. Chin, "Spatial reuse strategy in mmWave WPANs with directional antennas," *GLOBECOM - IEEE Global Telecommunications Conference*, pp. 5392–5397, 2012.

[20] C. S. Sum, Z. Lan, R. Funada, J. Wang, T. Baykas, M. A. Rahman, and H. Harada, "Virtual time-slot allocation scheme for throughput enhancement in a millimeter-wave multi-Gbps WPAN system," *IEEE Journal on Selected Areas in Communications*, vol. 27, no. 8, pp. 1379–1389, 2009.

[21] I. K. Son, S. Mao, M. X. Gong, and Y. Li, "On frame-based scheduling for directional mmWave WPANs," in *Proceedings - IEEE INFOCOM*, 2012, pp. 2149–2157.

[22] T. Korakis, G. Jakllari, and L. Tassiulas, "A {MAC} protocol for full exploitation of directional antennas in ad-hoc wireless networks," *ACM Int. Symposium on Mobile Ad-Hoc Networking & Computing*, pp. 98–107, 2003.

[23] E. Shihab, S. Member, L. Cai, J. Pan, and S. Member, "A Distributed Asnchronous Directional-to-Directional MAC Protocol for Wireless Ad Hoc Networks," *Ieee Tvt*, vol. 58, no. 9, pp. 5124–5134, 2009.

[24] H. Shokri-Ghadikolaei, C. Fischione, G. Fodor, P. Popovski, and M. Zorzi, "Millimeter wave cellular networks: A MAC layer perspective," *IEEE Transactions on Communications*, vol. 63, no. 10, pp. 3437–3458, 2015.

[25] T. Korakis, G. Jakllari, and L. Tassiulas, "CDR-MAC: A protocol for full exploitation of directional antennas in ad hoc wireless networks," *IEEE Transactions on Mobile Computing*, vol. 7, no. 2, pp. 145–155, 2008.

[26] Y. Niu, Y. Li, D. Jin, L. Su, and D. Wu, "Blockage robust and efficient scheduling for directional mmwave wpans," *IEEE Transactions on Vehicular Technology*, vol. 64, no. 2, pp. 728–742, 2015.

[27] "ISO/IEC/IEEE International Standard for Information technology–Telecommunications and information exchange between systems–Local and metropolitan area networks–Specific requirements-Part 11: Wireless LAN Medium Access Control (MAC) and Physical Layer (," pp. 1–634, 2014.

[28] Q. Chen, J. Tang, D. Wong, X. Peng, and Y. Zhang, "Directional cooperative MAC protocol design and performance analysis for IEEE 802.11ad WLANs," *IEEE Transactions on Vehicular Technology*, vol. 62, no. 6, pp. 2667–2677, 2013. [Online]. Available: https://www.scopus.com/inward/record.uri?eid=2-s2.0-84880527026&partnerID=40&md5=41429be7907ab8765148632b07e2ee30

[29] P. F. Smulders and A. G. Wagemans, "Frequency-domain measurement of the millimeter wave indoor radio channel," *IEEE Transactions on Instrumentation and Measurement*, vol. 44, no. 6, pp. 1017–1022, 1995.

[30] R. Kimura, R. Funada, Y. Nishiguchi, M. Lei, T. Baykas, C.-S. Sum, J. Wang, A. Rahman, Y. Shoji, H. Harada *et al.*, "Golay sequence aided channel estimation for millimeter-wave wpan systems," in *Personal, Indoor and Mobile Radio Communications, 2008. PIMRC 2008. IEEE 19th International Symposium on*. IEEE, 2008, pp. 1–5.

[31] T. Nitsche, C. Cordeiro, A. B. Flores, E. W. Knightly, E. Perahia, and J. C. Widmer, "IEEE 802.11ad: Directional 60 GHz communication for multi-Gigabit-per-second Wi-Fi [Invited Paper]," *IEEE Communications Magazine*, vol. 52, no. 12, pp. 132–141, 2014.

[32] T. Nitsche, C. Cordeiro, A. B. Flores, E. W. Knightly, E. Perahia, and I. N. P. Aper, "Radio Communications IEEE 802 . 11ad : Directional 60 GHz Communication for," no. December, pp. 132–141, 2014.